Journal of Sound and Vibration (2000) **237**(1), 101–118
doi:10.1006/jsvi.2000.3055, available online at http://www.idealibrary.com on IDEAL®

OUT-OF-PLANE VIBRATIONS OF SHEAR DEFORMABLE CONTINUOUS HORIZONTALLY CURVED THIN-WALLED BEAMS

MARCELO T. PIOVAN AND VÍCTOR H. CORTÍNEZ

Mechanical Systems Analysis Group, Universidad Tecnologica Nacional. F.R.B.B., 11 *de abril*, 461 -8000 *Bahía Blanca, Argentina*

AND

RAUL E. ROSSI

Department of Engineering, Universidad Nacional del Sur Avenida Alem, 1253-8000 *Bahía Blanca, Argentina*

(*Received* 25 *January* 1999, *and in final form* 28 *March* 2000)

This paper presents numerical study about the influence of the shear flexibility, due to either bending and warping, on the out-of-plane free vibration of continuous horizontally curved thin-walled beams with both open and closed sections. This study was made by means of a recently developed finite element formulation for shear deformable curved thin-walled beams. The model is briefly reviewed and is used to obtain natural frequencies of continuous I-beams and box beams. A parametric study was performed in order to elucidate the influence of shear deformability, on the dynamic behavior of continuous thin-walled curved beams, for different slenderness ratios, cross-sectional characteristics and boundary conditions.

1. INTRODUCTION

Many designers of engineering structures such as piping systems, highway bridges and machine elements take advantage of the high strength-to-weight ratio of thin-walled beams. Hence, extensive research on the dynamic behavior of these members has been made. Chidamparam and Leissa [1] classified most of the recent available papers concerning the dynamics of curved beams, some of them dealing with thin-walled beams. In the 1960s Vlasov [2] presented a dynamic theory of curved thin-walled beams, which was used successfully in several applications. Snyder and Wilson [3] used Vlasov's theory to study the dynamics of continuous curved thin-walled beams. They solved the equations by means of a closed-form solution, in order to provide numerical information for these structural members, which may be considered as a first approach in the design of highway, rail, rapid transit and guideway structures. Other researchers employed Vlasov's theory and used numerical approaches (like differential quadrature method) to find natural frequencies of thin-walled curved beams with open sections [4].

However, Vlasov's theory does not consider shear deformability which should have remarkable importance when vibrations associated with higher modes have to be determined. A few papers deal with vibrations of shear deformable curved thin-walled

0022-460X/00/410101 + 18 $35.00/0

beams. Kawakami *et al.* [5] studied the in-plane and out-of-plane vibrations of curved thin-walled considering shear effects associated to the lateral motion although neglecting the warping shear deformability. On the other hand, Fu and Hsu [6] analyzed statics of thin-walled beams taking into account warping shear effect, but not the bending shear flexibility. According to the author's knowledge there are only a few studies dealing with vibrations of curved thin-walled beams that consider the shear effect in a full form [7–9]. On the other hand, Piovan *et al.* [10] developed a theory which includes shear effects for the case of bisymmetrical H-sectional shape subjected to initial stresses. While the out-of-plane vibration analysis of curved thin-walled beams over multiple supports have been performed by many authors [3, 1–13], analysis including shear flexibility is, according to the authors' knowledge, non-existent.

The main objective of this paper is to elucidate the role of the shear flexibility, due to both bending and warping, on the out-of-plane free vibration behavior of continuous horizontally curved thin-walled beams with several end supports.

To accomplish this purpose a finite element formulation, recently developed by the authors [8, 10], for the dynamic analysis of shear flexible thin-walled curved beams is employed.

The present finite element solution is applied to uniform thin-walled curved beams with three spans of equal lengths. H-cross-sectional shape and rectangular closed sections are considered. The first six free-vibration frequencies and the corresponding mode shapes are calculated over a range of geometrical parameters such as horizontal radius of curvature and angular openings. A convergence study is also performed on the finite element employed in order to enhance its quality.

From the numerical study, conclusions are obtained with respect to the influence of the shear deformability for different slenderness ratios and cross-sectional characteristics.

2. MATHEMATICAL MODEL

The out-of-plane vibration for horizontally curved beams shown in Figure 1 is considered. As it may be seen, R denotes the radius of curvature at the centroid, L is the length of the beam between outer supports, e_A is the thickness of the walls, b and h are the width and height of the section, and α is the angle between outer supports. Also, it may be seen in Figure 1 that a right-hand co-ordinate system is used. Axes y and z are principal centroidal axes of the beam cross-section and x is tangent to the curved axis of this member. The assumptions of the model follow concepts of Cortinez *et al.* [8] and Cortinez and Rossi

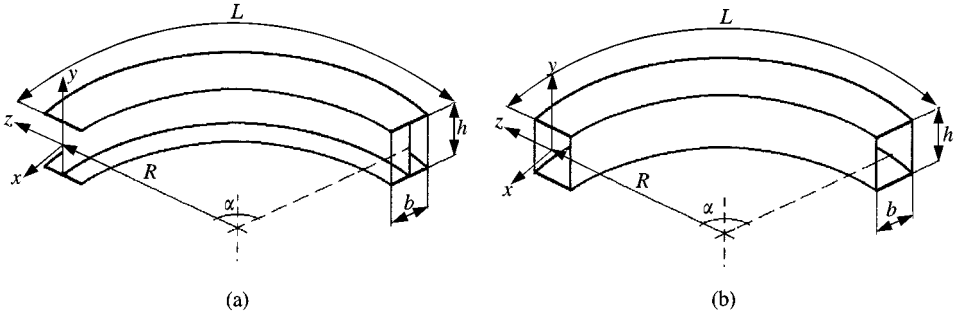

Figure 1. Analyzed beams: (a) H cross-section, (b) closed cross-section.

[14] and they are as follows. The original cross-section of the beam is preserved; the stress tensor is considered as a composition of a Saint Venant pure torsion state and a membranal state. The variation of curvature through the thickness is neglected for shear deformations. Then the displacement field can be written in the form [8]

$$u_x = -y\theta_z(x, t) + \omega(\theta(x, t) + \theta_z(x, t)/R),$$

$$u_y = v_c(x, t) - z\phi(x, t), \qquad u_z = y\phi(x, t), \tag{1}$$

where v_c is the vertical displacement of the centroid, ϕ is the torsional rotation, θ_z is the flexural rotation around the centroidal axis z, θ is a measure of the warping along the beam, ω is the warping function given by expressions (2) and (3) for the H-cross-section and rectangular closed section respectively [2, 15]:

$$\omega = D - \int_0^s r\,\mathrm{d}s \quad \text{with } D = \frac{1}{m}\int_0^m \mathrm{d}s \int_0^s r\,\mathrm{d}s, \qquad \omega = \oint (r - \psi)\,\mathrm{d}s, \tag{2, 3}$$

where r is the distance from the shear center to the tangent at a point in the middle line of the wall, m is the length of the cross-sectional thin wall and ψ is the shear strain due to Saint Venant torsion normalized with respect to $\mathrm{d}\phi/\mathrm{d}x$ according to Krenk and Gunneskov [15]. It has to be noted that expressions (1) reduce to Vlasov's displacement field used by Yang and Kuo [16] if the internal restraints $\theta_z = \partial v_c/\partial x$ and $\theta = \partial\phi/\partial x$ are predetermined. Therefore, the present model contains Vlasov's theory as a special case. When the restraints mentioned above are not imposed the shearing strain components are not zero in the middle line of the walls, as indicated by Cortínez and Rossi [8]. Thus the model allows shear deformability. The derivation of present model may be followed in a detailed form in references [8, 10].

The differential equations, which govern the out-of plane free vibration of the curved beam are [8]

$$-\frac{\partial Q_y}{\partial x} + \rho A\ \frac{\partial^2 v_c}{\partial t^2} = 0, \tag{4}$$

$$\frac{\partial M_z}{\partial x} - Q_y - \frac{1}{R}\ \frac{\partial B}{\partial x} + \frac{T_{sv}}{R} + \rho\left[I_z\ \frac{\partial^2\theta_z}{\partial t^2} + \frac{C_w}{R}\ \frac{\partial^2\theta}{\partial t^2}\right] = 0, \tag{5}$$

$$-\frac{\partial B}{\partial x} - T_w + \rho\left[C_w\frac{\partial^2\theta}{\partial t^2} + \frac{C_w}{R}\ \frac{\partial^2\theta_z}{\partial t^2}\right] = 0, \qquad -\frac{\partial(T_w + T_{sv})}{\partial x} + \frac{M_z}{R} + \rho I_0\ \frac{\partial^2\phi}{\partial t^2} = 0, \tag{6, 7}$$

where Q_y, M_z, B, T_w and T_{sv} denote shear force, bending moment, bimoment, flexural-torsional moment and Saint Venant torsion moment respectively. These generalized stresses are expressed in terms of the generalized displacement (1) as

$$Q_y = GK_y\left(\frac{\partial v_c}{\partial x} - \theta_z\right), \qquad M_z = -EI_z\left(\frac{\partial\theta_z}{\partial x} - \frac{\phi}{R}\right), \tag{8a, b}$$

$$B = EC_w\ \frac{\partial}{\partial x}\left(\theta + \frac{\theta_z}{R}\right), \qquad T_w = GK_w\left(\frac{\partial\phi}{\partial x} - \theta\right), \tag{8c, d}$$

$$T_{sv} = GJ\left(\frac{\partial\phi}{\partial x} + \frac{\theta_z}{R}\right), \tag{8e}$$

where A is the cross-sectional area, I_z and I_y are moments of inertia with respect to axes x and y, respectively, C_w is the warping constant, J is the torsion constant, I_0 is the polar moment of inertia and K_y and K_w are shear rigidity factors deduced by Cortinez and Rossi [14, 17].

The boundary conditions at a simple support are zero vertical deflection ($v_c = 0$), zero torsional rotation ($\phi = 0$), zero flexural moment ($M_z = 0$) and zero bimoment ($B = 0$), although taking into account equations (8b,c) they can be expressed in condensed form in equation (9). For a clamped support the boundary conditions are shown in expression (10):

$$v_c = \phi = \frac{\partial \theta_z}{\partial x} = \frac{\partial \theta}{\partial x} = 0, \qquad v_c = \phi = \theta_z = \theta = 0. \tag{9, 10}$$

A finite element based on the present model was developed in references [8, 10]. This element may be considered a generalization for curved beams of an earlier finite developed for straight beams by Cortinez and Rossi [14]. The vector that contains the nodal unknowns is denoted by q and it is

$$q = \{v_{c1}, \theta_{z1}, \phi_1, \theta_1, v_{c2}, \theta_{z2}, \phi_2, \theta_2\}^{\mathrm{T}}. \tag{11}$$

For the out-of-plane vibration displacement field may be interpolated as indicated by equations (12a–d), where coefficients b_i and d_i are indeterminate functions depending on time:

$$v_c = b_0 + b_1\tilde{x} + b_2\tilde{x}^2 + b_3\tilde{x}^3, \qquad \theta_z = b_1 + \frac{\beta_1 b_3}{2} + 2b_2\tilde{x} + 3b_3\tilde{x}^2, \tag{12a, b}$$

$$\phi = d_0 + d_1\tilde{x} + d_2\tilde{x}^2 + d_3\tilde{x}^3, \qquad \theta = d_1 + \frac{\beta_3 d_3}{2} + 2d_2\tilde{x} + 3d_3\tilde{x}^2, \tag{12c, d}$$

with

$$\tilde{x} = \frac{x}{l_e}, \qquad \beta_1 = \frac{12EI_z}{GK_y l_e^2}, \qquad \beta_3 = \frac{12EC_W}{GK_w l_e^2}, \tag{13}$$

where l_e is the element length. The element interpolated with the displacement field (12a–d) is shear locking free and it could be reduced, as a limiting case, to a Vlasov element [8, 10]. This is possible when a large shear rigidity (say K_w, $K_y \to 10^{20}$) is imposed in the stiffness matrix, and on the other hand, when flexure and warping rotary inertias are neglected (say $C_W = I_z = 0$) in the mass matrix. Also, this curved element reduces to the straight beam finite element of Cortínez and Rossi [14] when $R \to \infty$.

Carrying out the conventional steps of the finite element method for free-vibration problems, one arrives at the expression

$$[\mathbf{K} - \Omega^2\mathbf{M}]\mathbf{Q}^* = \mathbf{0}, \tag{14}$$

where $\mathbf{K}$ is the global matrix, $\mathbf{M}$ is the global mass matrix, $\mathbf{Q}^*$ is the displacement vector independent of time, $\Omega = 2\pi f$ is the circular frequency of vibration and f is the frequency (measured in Hz).

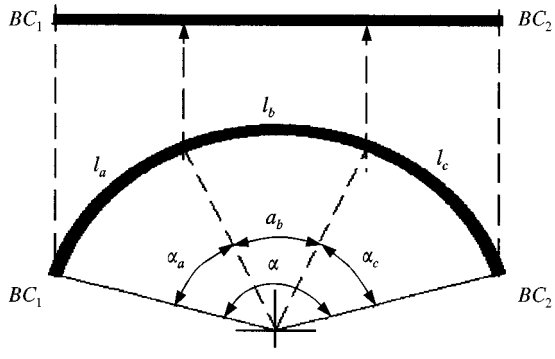

Figure 2. Diagram of the continuous beam studied, with the boundary conditions (BC_i) considered l_a, l_b, l_c, α_a, α_b, α_c are lengths and subtended angles of each span. α is the subtended angle between outer supports.

TABLE 1

Properties of the sections used in the numerical studies

Property	Open H-section	Closed-section
Cross-sectional area: A (m^2)	2·40E − 02	2·40E − 02
Inertia moment: I_z (m^4)	7·47E − 04	5·33E − 04
Polar moment: I_0 (m^4)	9·61E − 04	7·20E − 04
Warping constant: C_w (m^6)	8·55E − 06	3·53E − 07
Torsion constant: J (m^4)	3·20E − 06	4·26E − 04
Flexural shear rigidity factor: K_y (m^2)	7·03E − 03	1·46E − 02
Torsion shear rigidity factor: K_w (m^4)	5·54E − 04	5·33E − 05
Longitudinal modulus of elasticity: E (N/m^2)	2·10E + 11	2·10E + 11
Transversal modulus of elasticity: G (N/m^2)	8·07E + 10	8·07E + 10
Mass density: ρ (kg/m^3)	7830	7830

3. GEOMETRICAL MODELS

A general diagram of the continuous beam studied here is shown in Figure 2. It consists of three circular spans of length l_a, l_b, l_c (thus, $L = l_a + l_b + l_c$), with four supports, where the inner ones are simply supported and the outer ones may be simply supported or clamped. For this general outline, two particular cases of outer boundary conditions were selected: simply supported at both ends (SS–SS) and clamped at both ends (C–C). The spans have equal length ($l_a = l_b = l_c$). The dimensions for the open section H were $b = h = 0{\cdot}40$ m, whereas for the boxed rectangular section $b = h/2 = 0{\cdot}20$ m. For both sections the same wall thickness $e_A = 0{\cdot}02$ m were employed. The material properties for both sections as well as sectional features are listed in Table 1.

4. NUMERICAL RESULTS

4.1. CONVERGENCE CHECK

In order to check the element performance, a set of comparative tests was performed with analytical results, as well as convergence studies. In Table 2, a convergence check of the first six frequencies (measured in Hz) is given for the outer boundary conditions SS–SS with

TABLE 2

Convergence checks of the first six frequencies (Hz). Results with shear flexibility are depicted in column (a). *Results without shear flexibility in column* (b)

Column a	$\alpha = 45^\circ$ $R = 2$ m				Column b	$\alpha = 45^\circ$ $R = 2$ m			
	Elements			Analytical		Elements			Analytical
f	21	45	81	[9]	f	21	45	81	[9]
1	1567·79	1559·17	1557·53	1557·17	1	2391·58	2391·60	2390·79	2395·49
2	1576·27	1568·34	1566·65	—	2	3058·87	3058·84	3057·80	—
3	1585·68	1577·13	1575·50	—	3	3639·47	3639·47	3639·57	3633·01
4	1768·83	1761·14	1760·01	1759·21	4	4396·88	4396·57	4395·12	—
5	1846·58	1838·54	1837·02	—	5	4539·27	4539·17	4539·31	—
6	2041·15	2030·72	2028·73	—	6	6309·17	6308·54	6308·68	—
	$\alpha = 90^\circ$ $R = 4$ m					$\alpha = 90^\circ$ $R = 4$ m			
f	21	45	81	[9]	f	21	45	81	[9]
1	138·61	137·57	137·31	137·24	1	145·07	145·08	145·03	145·06
2	192·31	191·32	191·12	—	2	219·01	219·02	218·93	—
3	287·57	286·24	286·09	—	3	337·31	337·29	337·15	—
4	309·81	308·91	308·69	308·58	4	378·54	378·56	378·53	378·45
5	327·85	326·80	326·54	—	5	445·43	445·45	445·43	—
6	367·24	365·76	365·47	—	6	605·57	605·56	605·56	—
	$\alpha = 120^\circ$ $R = 8$ m					$\alpha = 120^\circ$ $R = 8$ m			
f	21	45	81	[9]	f	21	45	81	[9]
1	12·99	12·38	12·25	12·18	1	12·26	12·26	12·26	12·26
2	29·55	29·13	29·04	—	2	30·36	30·35	30·35	—
3	53·32	52·81	52·70	—	3	55·58	55·56	55·56	—
4	87·35	85·81	85·47	85·31	4	88·14	88·06	88·06	88·06
5	101·68	101·29	101·20	—	5	105·14	105·14	105·15	—
6	105·83	104·47	104·18	—	6	110·53	110·43	110·42	—

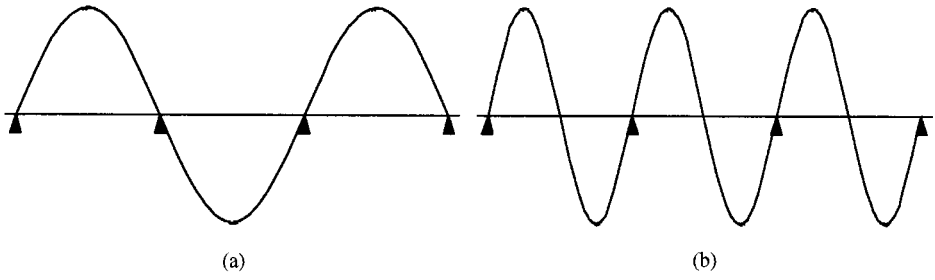

Figure 3. Modes of the analytical results taken from reference [9]: (a) third frequency of a single-span beam, (b) sixth frequency of a single span beam.

TABLE 3

Comparisons with non-dimensional frequencies: I, *reference* [3]; II, *present model*

α (deg)	Parameters	Model	p_1	p_2	p_3	p_4	p_5	p_6
45	$C = 0{\cdot}05$	I	0·975	1·265	1·861	3·987	4·548	5·584
	$\xi = 0{\cdot}005$	II	0·976	1·265	1·862	3·988	4·548	5·584
	$D = 0{\cdot}001$	$\lvert p_{i(II)} - p_{i(I)}\rvert / p_{i(I)}$ (%)	0·10	0·00	0·05	0·03	0·00	0·00
	$C = 2$	I	0·992	1·275	1·866	3·993	4·552	5·587
	$\xi = 0{\cdot}005$	II	0·992	1·275	1·866	3·993	4·552	5·587
	$D = 0{\cdot}01$	$\lvert p_{i(II)} - p_{i(I)}\rvert / p_{i(I)}$ (%)	0·00	0·00	0·00	0·00	0·00	0·00
90	$C = 0{\cdot}05$	I	0·844	1·166	1·798	3·901	4·477	5·529
	$\xi = 0{\cdot}005$	II	0·845	1·167	1·798	3·903	4·479	5·531
	$D = 0{\cdot}001$	$\lvert p_{i(II)} - p_{i(I)}\rvert / p_{i(I)}$ (%)	0·11	0·09	0·00	0·05	0·04	0·03
	$C = 2$	I	0·967	1·254	1·850	3·968	4·530	5·567
	$\xi = 0{\cdot}005$	II	0·967	1·254	1·850	3·968	4·530	5·568
	$D = 0{\cdot}01$	$\lvert p_{i(II)} - p_{i(I)}\rvert / p_{i(I)}$ (%)	0·00	0·00	0·00	0·00	0·00	0·02
180	$C = 0{\cdot}05$	I	0·523	0·899	1·568	3·377	4·030	5·157
	$\xi = 0{\cdot}005$	II	0·523	0·899	1·569	3·381	4·034	5·160
	$D = 0{\cdot}001$	$\lvert p_{i(II)} - p_{i(I)}\rvert / p_{i(I)}$ (%)	0·00	0·00	0·06	0·12	0·10	0·06
	$C = 2$	I	0·866	1·171	1·785	3·866	4·438	5·486
	$\xi = 0{\cdot}005$	II	0·866	1·171	1·785	3·866	4·438	5·486
	$D = 0{\cdot}01$	$\lvert p_{i(II)} - p_{i(I)}\rvert / p_{i(I)}$ (%)	0·00	0·00	0·00	0·00	0·00	0·00

several values of angular spacing α. Comparisons were carried out with analytical results obtained with the methodology used in reference [9] (for a single span curved H-beam with the same outer angular spacing α). The Column 'a' shows results allowing shear flexibility whereas Column 'b' shows results without shear flexibility, but allowing rotary inertia. As it may be appreciated, convergence is good enough even with 21 element, i.e., seven elements over each span. In Table 2 the frequencies, which were compared with the analytical method [9], have the sinusoidal modes shown in Figures 3(a) and 3(b) respectively. These two modes are referred to the vertical displacement v_c and they correspond, respectively, to the third and sixth modes of the single span curved H-beam studied in reference [9].

4.2. COMPARISON WITH VLASOV MODELS

In Table 3 comparisons with the non-dimensional frequencies (actually $p_i = \Omega\sqrt{(\rho A l_a^4)/(\pi^4 E I_z)}$) of reference [3] are presented. Results are given for outer angular

spacing (α) of 45, 90 and 180° (i.e., 15, 30 and 60° on each span) and with the outer boundary conditions SS–SS. It is important to point out that the mathematical model studied in reference [3] is the classical Vlasov model for curved beams, i.e., a model that does not allow rotary inertia and shear flexibility, moreover these equation were solved with a closed-form solution.

For each angular spacing, two different sets of the dimensionless parameter $\{C, \xi, D\}$ (which are defined in reference [3]) were selected. Then $C = GJ/(EI_z)$ is the ratio between the torsional and flexural rigidities, $\xi = r_p/R$ is the ratio between the polar radius of gyration and the horizontal radius of curvature and finally $D = EC_w/(EI_zR^2)$ is a parameter related to warping and flexible rigidities.

In order to reproduce frequencies as accurately as possible a large number of elements was adopted for each calculation. Therefore, models with 81 elements without shear flexibility were prepared for this task. Then in Table 3, it is possible to see an excellent matching in all the cases performed, and the maximum error is 0·12%.

4.3. OPEN H-CROSS SECTION

In Tables 4 and 5 the frequencies for the case of an open H-cross-section are presented. For these tables, the frequencies were obtained with models of 81 elements of equal length. In these tables results calculated with the shear flexible model and the Vlasov model are shown. Table 4 depicts the first frequencies (Hz) for values of $\alpha = 90$ and 120°, with outer boundary conditions SS–SS, whereas Table 5 shows the frequencies for the aforementioned angles but with outer supports C–C.

With the purpose to evaluate the influence of the shear effect on the free vibrational behavior of the structural members studied, the following quantity $\varepsilon\ (\%) = |f_{Vlasov} - f_{shear}|/f_{shear}$ is defined as a measure of the difference between the model accounting for shear

TABLE 4

Frequencies (Hz) for beams with an H cross-section and SS–SS outer boundary conditions: I, *allowance for shear flexibility, rotary and warping inertia*, II, *Vlasov model*

α (deg)	h/R	Case	f_1	f_2	f_3	f_4	f_5	f_6
90	0·200	I	519·21	603·73	738·77	767·79	797·64	903·04
		II	645·42	877·16	1309·61	1389·33	1729·87	2477·68
	0·100	I	137·31	191·06	286·01	308·69	326·54	365·41
		II	147·66	222·58	342·34	388·43	459·35	629·81
	0·050	I	29·83	53·21	88·83	119·67	126·29	142·21
		II	30·39	56·74	94·82	128·15	139·71	170·62
	0·025	I	5·95	13·62	24·79	40·14	49·86	50·93
		II	5·96	13·92	25·51	40·85	51·39	51·85
120	0·200	I	282·38	366·02	511·04	565·16	587·06	648·81
		II	327·19	487·62	750·91	853·07	1021·21	1415·31
	0·100	I	64·26	109·26	179·67	234·68	244·86	268·04
		II	67·11	124·00	205·43	270·53	299·45	375·48
	0·050	I	12·25	29·04	52·70	85·47	101·20	104·18
		II	12·31	30·49	55·85	88·92	105·36	111·35
	0·025	I	2·36	6·75	12·88	19·57	27·27	35·99
		II	2·36	6·84	13·09	19·72	27·94	37·02

TABLE 5

Frequencies (Hz) for beams with an H cross-section and C–C outer boundary conditions: I, *allowance for shear flexibility, rotary and warping inertia*, II, *Vlasov model*

α (deg)	h/R	Case	f_1	f_2	f_3	f_4	f_5	f_6
90	0·200	I	603·73	738·77	797·64	799·96	903·04	990·23
		II	877·15	1309·61	1593·28	1729·87	2477·68	2989·80
	0·100	I	191·06	286·01	326·54	338·48	365·41	388·73
		II	222·58	342·34	417·40	459·35	629·81	753·42
	0·050	I	53·21	88·83	111·07	126·29	142·21	152·21
		II	56·74	94·82	118·72	139·71	170·62	196·68
	0·025	I	13·62	24·79	33·75	49·86	52·12	55·33
		II	13·92	25·51	35·14	51·39	53·37	57·54
120	0·200	I	366·02	511·04	575·74	587·06	648·81	704·21
		II	487·62	750·91	918·30	1021·21	1415·31	1696·38
	0·100	I	109·26	179·67	221·16	224·86	268·04	282·74
		II	124·00	205·43	256·15	299·45	375·48	437·59
	0·050	I	29·04	52·70	70·70	103·57	104·18	110·65
		II	30·49	55·85	76·31	109·25	111·35	120·28
	0·025	I	6·75	12·88	19·54	27·27	35·99	42·44
		II	6·84	13·09	20·19	27·94	37·02	43·92

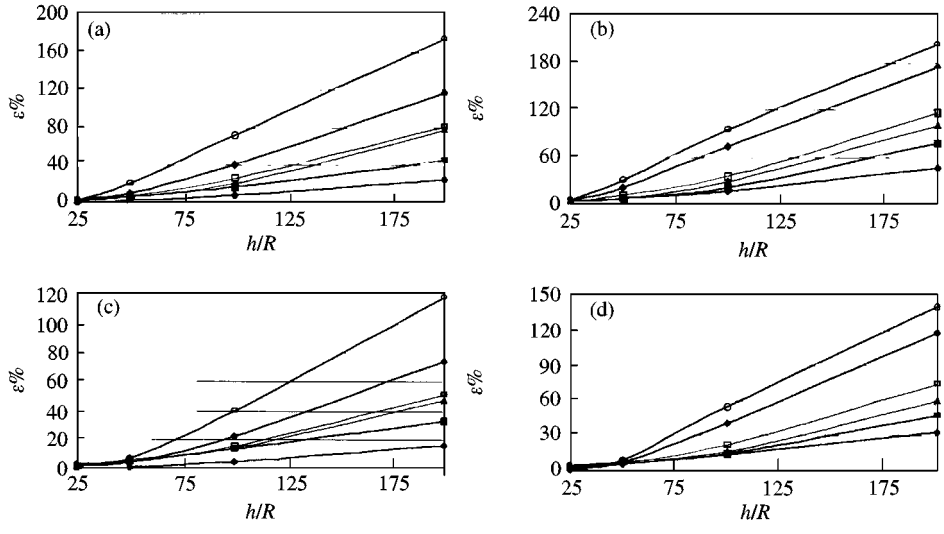

Figure 4. Curves of error versus relation h/R for the cases of Tables 4 and 5: (a) Case 90° of Table 4, (b) Case 90° of Table 5, (c) Case 120° of Table 4, (d) Case 120° of Table 5; ε%: percent difference; h/R: height–radius ratio. (–◆–, First frequency; –■–, second frequency; –▲–, third frequency; –□–, fourth frequency; –◇–, fifth frequency; –○–, sixth frequency.)

flexibility and the Vlasov's model. The curves of ε versus h/R for each frequency number of Table 4 and 5 are presented in Figure 4. As it could be clearly seen in Figure 4, for a given H-cross-section, the differences between frequencies calculated by Vlasov's model and the model including shear flexibility rise uniformly with the ratio h/R. These curves show how

significant is the shear effect on the dynamics of thin-walled open beams. For example, the first frequency of a deep beam, corresponding to $h/R = 0{\cdot}200$ and $\alpha = 90^\circ$ with clamped ends, has a difference of $\varepsilon = 45\%$ (Figure 4(b)), but the sixth frequency of the same case has a difference of $\varepsilon = 202\%$. However, in the case of slender beams, say $h/R = 0{\cdot}025$ and lower, these differences are small (less than 3%) for all the frequencies considered.

4.4. CLOSED CROSS-SECTION

In Tables 6 and 7 the frequencies for the case of closed-rectangular cross-section are presented. These tables exhibit the same pattern as the previous ones, except for the box section described in Table 1. Thus, Table 6 shows the frequencies (Hz) for the values of α of 90 and 180°, with SS–SS outer boundary conditions, whereas Table 7 shows the frequencies for the angles mentioned above but with C–C outer supports.

In Figure 5, it is possible to see curves of ε versus h/R for the six frequencies of Table 6 and 7. Differences between Vlasov and present models are noticeable. For example, the third frequency in Figure 6(a) has $\varepsilon = 34\%$ at $h/R = 0{\cdot}100$, but the sixth frequency in Figure 5(b) has $\varepsilon = 99\%$ at $h/R = 0{\cdot}200$. However, observing Figure 5 and comparing it with Figure 4, one may see a very different influence of the shear effect on the dynamics of curved beams with rectangular closed sections. Some frequencies have a uniform increase of ε with h/R and some other have different behavior. In fact, for a given frequency number, ε may increase with h/R in the whole range, like for example f_1, f_2 and f_3 in Figure 5(c), however for other frequencies ε could decrease after certain values of h/R, like f_3 in Figure 5(b) or f_4, f_5 and f_6 in Figures 5(c) and 5(d). The explanation of this behavior is related to the qualitative and quantitative variation, with h/R, of the mode characteristics for a given frequency number. A coupled flexural-torsional mode of the frequency could change to a dominant torsional mode (where, for a closed section the warping is negligible) depending on the

TABLE 6

Frequencies (Hz) for beams with closed cross-section and SS–SS outer boundary conditions: I, *allowance for shear flexibility, rotary and warping inertia*, II, *Vlasov model*

α (deg)	h/R	Case	f_1	f_2	f_3	f_4	f_5	f_6
90	0·200	I	733·84	811·89	976·16	1236·26	1242·53	1255·64
		II	922·78	1114·88	1279·17	1387·89	1540·18	2080·14
	0·100	I	229·76	279·52	374·17	617·05	619·16	623·44
		II	253·09	331·75	488·50	627·65	635·56	657·12
	0·050	I	62·34	79·95	114·87	242·36	267·35	308·35
		II	64·10	84·22	125·61	270·05	307·87	309·24
	0·025	I	15·95	20·83	30·75	65·75	74·37	89·97
		II	16·07	21·12	31·50	67·78	77·53	95·49
180	0·200	I	189·33	248·38	355·14	682·41	684·19	688·04
		II	202·75	287·21	447·04	716·90	725·01	746·58
	0·100	I	51·13	70·91	108·24	229·83	256·37	302·00
		II	52·16	74·18	117·18	253·09	292·42	347·44
	0·050	I	13·07	18·46	28·90	62·35	71·33	87·30
		II	13·13	18·68	29·53	64·09	74·17	92·37
	0·025	I	3·28	4·66	7·36	15·95	18·41	22·82
		II	3·29	4·68	7·40	16·07	18·59	23·16

TABLE 7

Frequencies (Hz) for beams with closed cross-section and C–C outer boundary conditions: I, *allowance for shear flexibility, rotary and warping inertia*, II, *Vlasov model*

α (deg)	h/R	Case	f_1	f_2	f_3	f_4	f_5	f_6
90	0·200	I	811·89	976·16	1067·47	1242·53	1255·64	1262·95
		II	1113·85	1277·49	1325·59	1540·18	2080·14	2498·71
	0·100	I	279·52	374·17	425·21	619·16	623·44	625·63
		II	331·75	488·50	576·98	635·56	657·12	687·22
	0·050	I	79·95	114·87	136·24	267·35	309·01	310·41
		II	84·22	125·61	153·32	307·87	310·86	315·34
	0·025	I	20·83	30·75	37·23	74·37	89·97	99·36
		II	21·12	31·50	38·47	77·53	95·49	106·89
180	0·200	I	248·38	355·14	412·82	684·19	688·04	690·78
		II	287·21	447·04	545·01	724·43	745·98	773·03
	0·100	I	70·91	108·24	131·24	256·37	302·00	326·86
		II	74·18	117·18	146·16	292·42	348·32	352·53
	0·050	I	18·46	28·90	35·76	71·33	87·30	96·95
		II	18·68	29·53	36·86	74·17	92·37	103·98
	0·025	I	4·66	7·36	9·16	18·41	22·82	25·59
		II	4·68	7·40	9·23	18·59	23·16	26·07

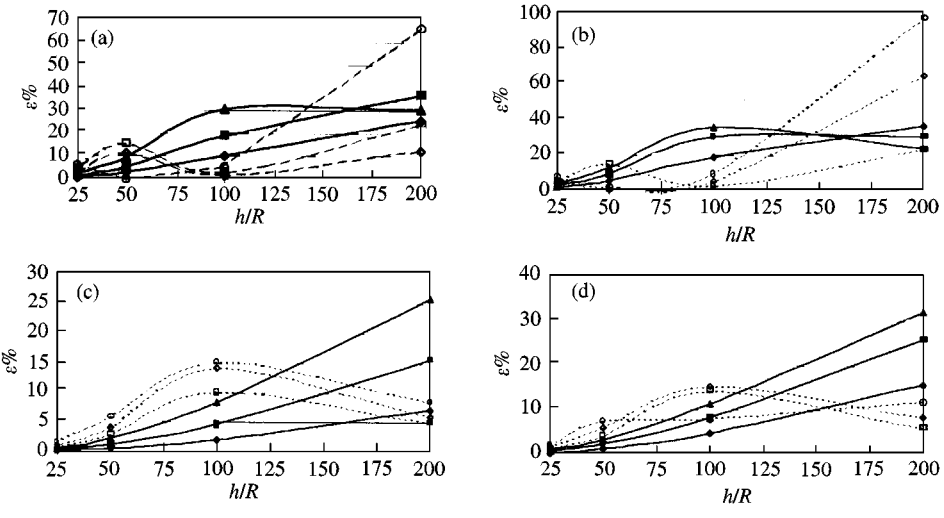

Figure 5. Curves of error versus relation h/R for the cases of Tables 6 and 7: (a) Case 90° of Table 6, (b) Case 90° of Table 7, (c) Case 180° of Table 6, (d) Case 180° of Table 7; ε%: percent difference; h/R: height–radius ratio. (–◆–, First frequency; –■–, second frequency; –▲–, third frequency; –□–, fourth frequency; –◇–, fifth frequency; –○–, sixth frequency.)

values of h/R for a particular frequency number and geometrical features. Actually, in Figures 5(c) and (5d) it is possible to appreciate a very different behavior beyond $h/R = 0{\cdot}100$ in frequencies f_4, f_5 and f_6. These frequencies have basically a coupled flexural-torsional motion, but for $h/R = 0{\cdot}200$, the motion changes to a predominant torsional mode.

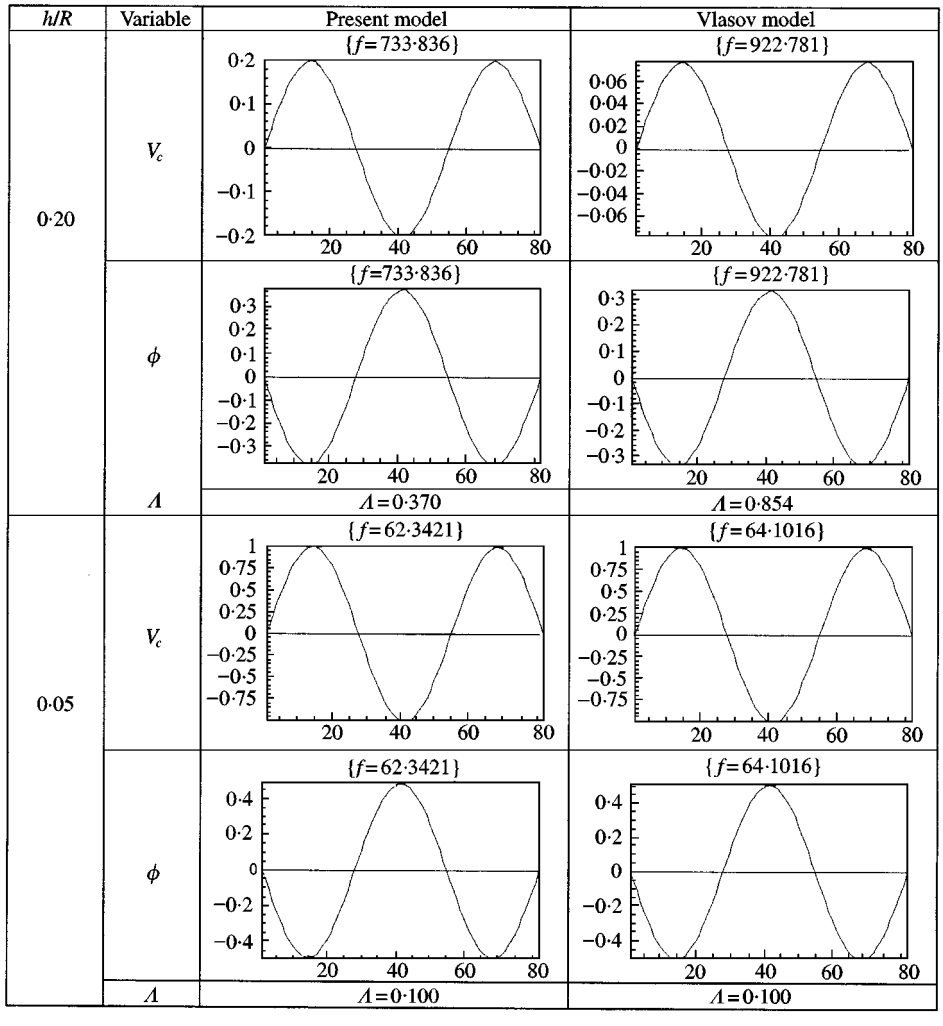

Figure 6. Mode shapes of the first frequency (f_1) for the beam with closed section, $\alpha = 90^\circ$ and SS–SS outer boundary conditions Λ: measure of motion characteristics; v_c: vertical displacement, ϕ: torsion angle.

Unlike what occurs in the thin-walled open sections, thin-walled closed sections do not manifest a quite considerable difference between Vlasov and present models, when the motion is predominantly torsional. In order to explain the behavior of ε in Figures 5(a)–5(d), the non-dimensional parameter $\Lambda = |h/2\,\phi_{max}/v_{cmax}|$ is defined as a measure of the motion characteristics for a given frequency. That is, values of Λ quite greater than one reveal dominant torsional modes, values of Λ closer to zero correspond to dominant flexural modes, values of Λ belonging to the interval (0·1, 1·0) may be accepted as coupled flexural-torsional modes.

Figures 6–11 depict a sequence of mode shapes at some frequencies showing the aforementioned qualitative and quantitative variation. Thus, Figures 6–8 show the mode shapes of variables v_c, ϕ and the corresponding parameter Λ for frequencies f_1, f_2 and f_3, respectively, calculated with both models, the case of $\alpha = 90^\circ$ with SS–SS outer boundary conditions, for $h/R = 0{\cdot}05$ and 0·20. Then in Figures 6–8, it is possible to appreciate that, for

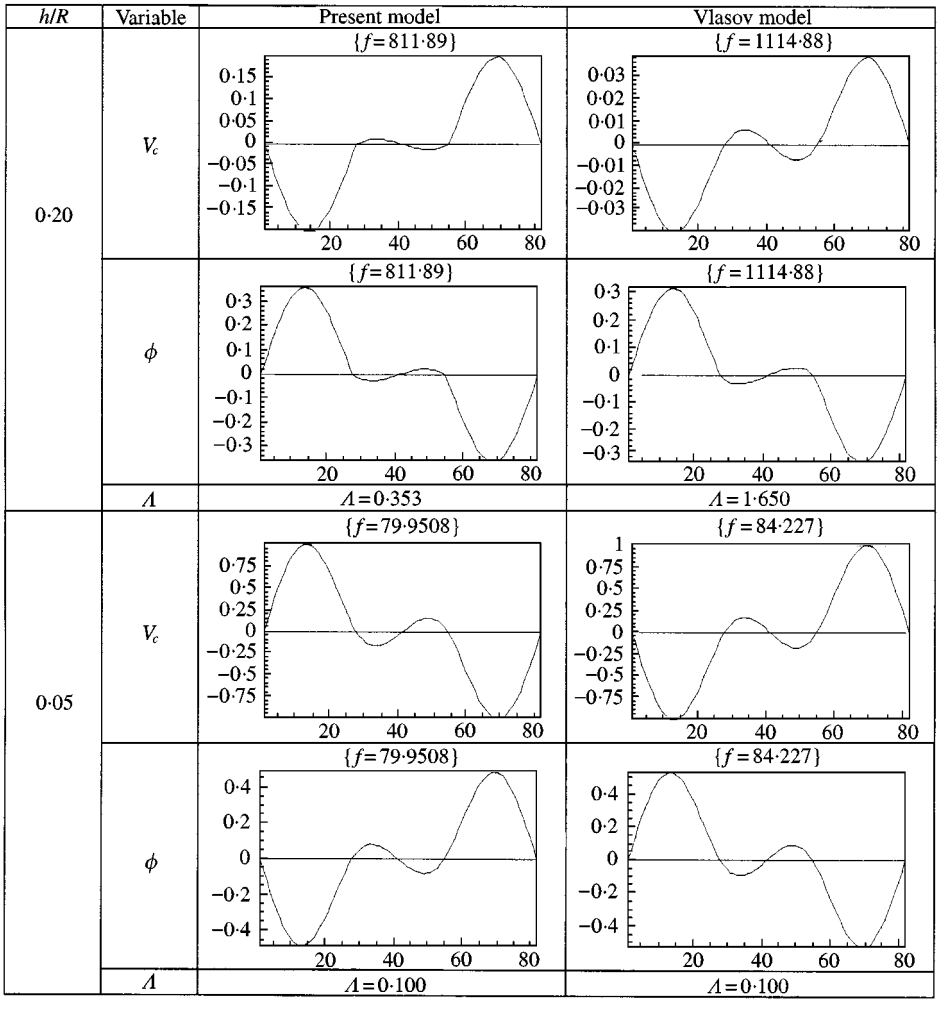

Figure 7. Mode shapes of the second frequency (f_2) for the beam with closed section, $\alpha = 90^\circ$ and SS–SS outer boundary conditions Λ: measure of motion characteristics; v_c: vertical displacement, ϕ: torsion angle.

a given frequency and a value of h/R, the mode shape of each variable is not different, and it is the same for both models. Just for instance, the mode shape of v_c in the present model is the same at $h/R = 0{\cdot}05$ and $0{\cdot}20$, it occurs also in the Vlasov model. However, quantitative differences appear in the Vlasov model for f_3 (Figure 8). This mode is flexural-torsional at $h/R = 0{\cdot}05$ (i.e., $\Lambda = 0{\cdot}320$) and it changes to a torsional-dominant mode at $h/R = 0{\cdot}20$ (i.e., $\Lambda = 5{\cdot}250$). With little differences, the same response could be observe in Figure 5(b), i.e., for the same angular opening but with C–C outer boundary conditions.

Figures 9–11 show the mode shapes of variables v_c, ϕ, and the corresponding parameter Λ for frequencies f_4, f_5 and f_6, respectively, calculated with Vlasov and present models, but for $\alpha = 180^\circ$, cases $h/R = 0{\cdot}10$ and $0{\cdot}20$ (Table 6). The mode shapes at these three frequencies change abruptly from a coupled flexural-torsional mode at $h/R = 0{\cdot}10$ (i.e., $\Lambda < 1$) in both models to a dominant torsional mode at $h/R = 0{\cdot}20$, except in the case of f_6 (Figure 11) where the Vlasov model already has a dominant mode at $h/R = 0{\cdot}10$ (i.e., $\Lambda = 8$).

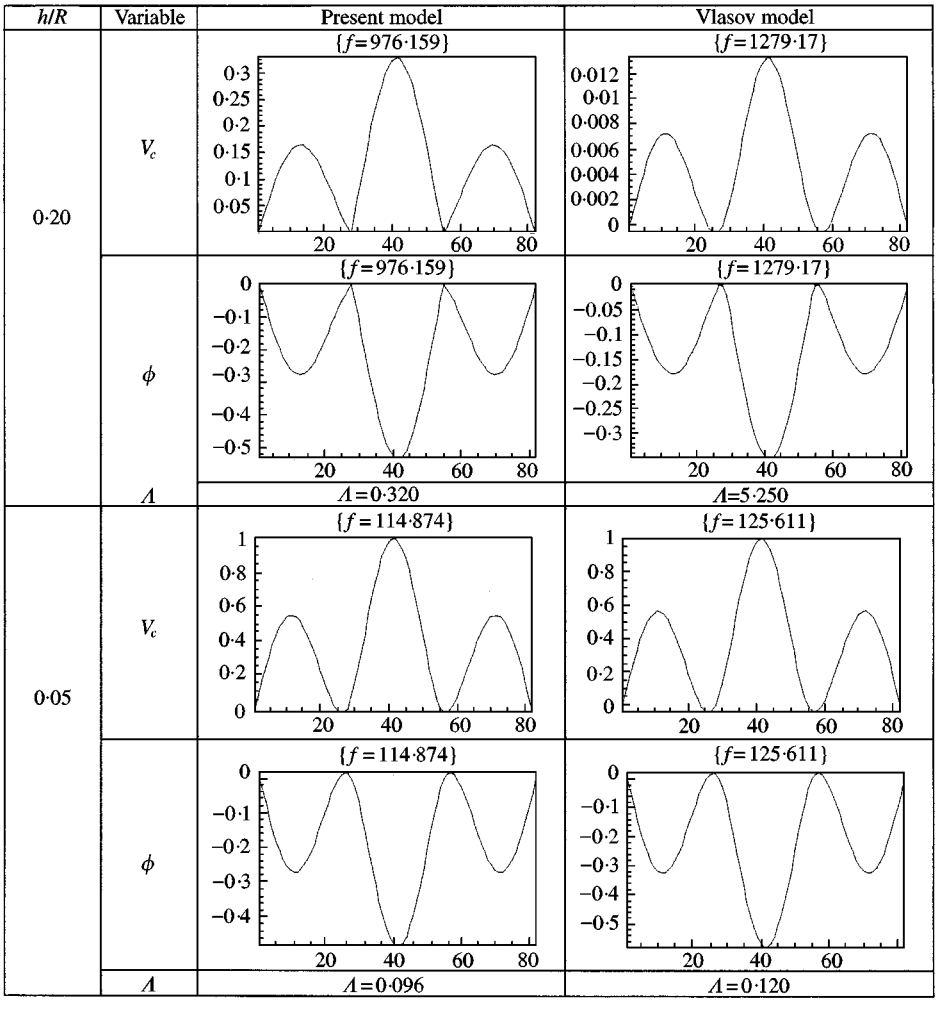

Figure 8. Mode shapes of the third frequency (f_3) for the beam with closed section, $\alpha = 90^\circ$ and SS–SS outer boundary conditions Λ: measure of motion characteristics; v_c: vertical displacement, ϕ: torsion angle.

Also, in this figure it is possible to see a change in the mode shape when one moves from $h/R = 0{\cdot}10$ to $0{\cdot}20$ for a given frequency number.

5. CONCLUSIONS

A finite element analysis of the out-of-plane vibrations of continuous thin-walled curved beams was performed. Special emphasis was given to the influence of the shear flexibility, due to bending and warping, over the dynamics of the member. The convergence analysis and the comparisons with exact results show the very good performance of the element employed.

It may be concluded from the present analysis that the shear effect is quite noticeable for frequencies associated with high modes or even with low modes in the case of deep beams.

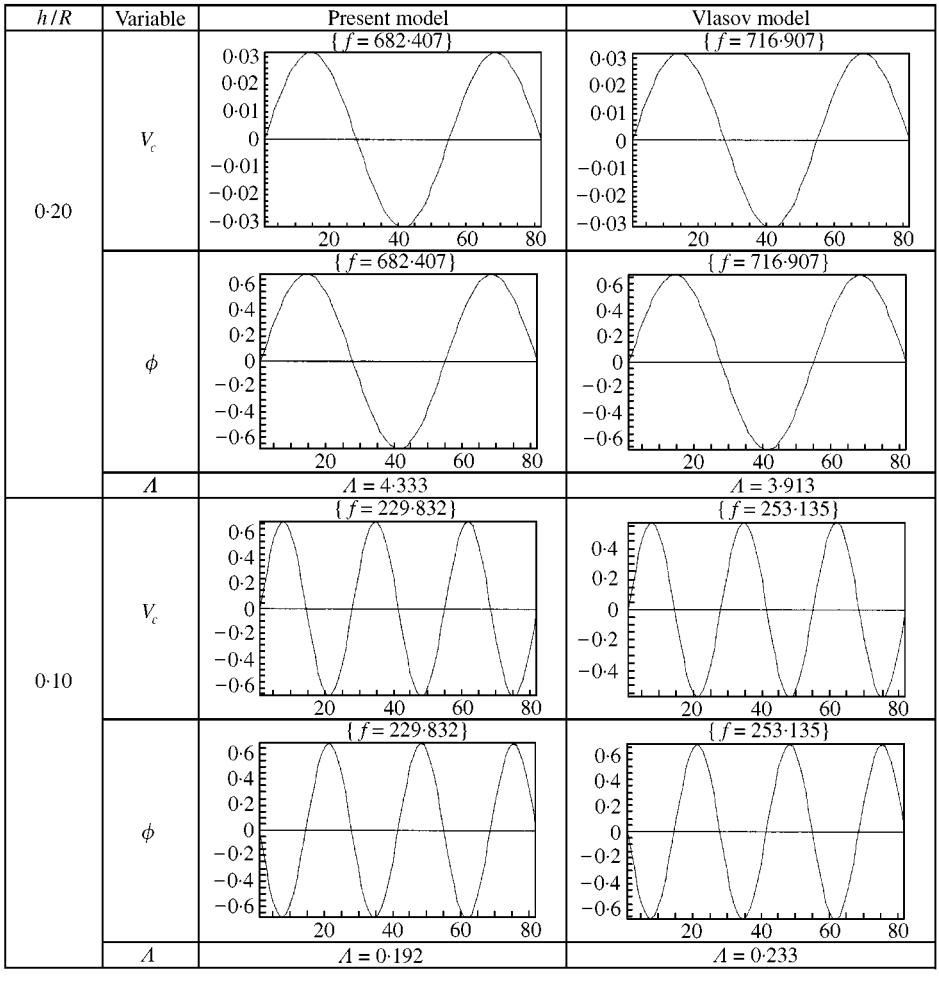

Figure 9. Mode shapes of the fourth frequency (f_4) for the beam with closed section, $\alpha = 180^\circ$ and SS–SS outer boundary conditions Λ: measure of motion characteristics; v_c: vertical displacement, ϕ: torsion angle.

Moreover, the shear effect showed different influences depending on the cross-section type, i.e., if the section is open or closed. The relative difference (ε) between frequencies obtained with Vlasov and present models, for the case of the H-open section, decreases uniformly with h/R (Figure 4). However, for the closed section, ε decreases uniformly with h/R only for certain frequencies but for other frequencies the variation of ε with h/R is connected with qualitative and quantitative changes in its dominant mode (which are distinguished by the introduced parameter Λ) especially when a flexural–torsional coupled mode changed to a torsional-dominant mode (Figures 9–11).

From the present study it should be concluded that the shear effect should be taken into account in the dynamic analysis of these types of structures at least when deep beams or high modes are considered.

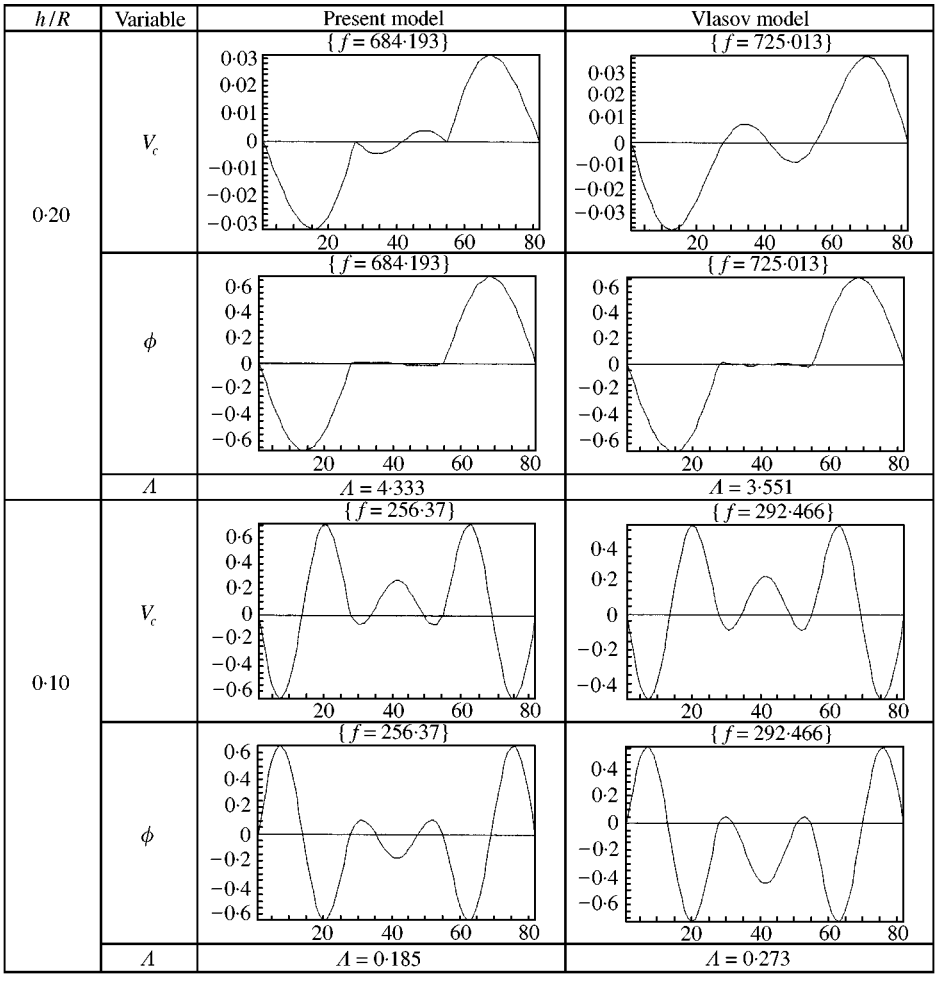

Figure 10. Mode shapes of the fifth frequency (f_5) for the beam with closed section, $\alpha = 180^\circ$ and SS–SS outer boundary conditions Λ: measure of motion characteristics; v_c: vertical displacement, ϕ: torsion angle.

ACKNOWLEDGMENT

The authors highly appreciate the support of Secretaria de Ciencia y Tecnología of Universidad Tecnológica Nacional and Secretaría de ciencia y Tecnologia of Universidad Nacional del Sur. The authors also thank the support of CONICET.

REFERENCES

1. P. CHIDAMPARAN and A. W. LEISSA 1993 *Applied Mechanics Reviews* **46**, 467–483. Vibrations of planar curved beams, rings and arches.
2. V. Z. VLASOV 1961 *Thin Walled Elastic Beams*. Washington, DC: 2° National Science Foundation.
3. J. M. SNYDER and J. F. WILSON 1992 *Journal of Sound and Vibration* **157**, 345–355. Free vibrations of continuous horizontally curved beams.
4. K. KANG, C. W. BERT and A. G. STRIZ 1996 *Journal of Structural Engineering* **122**, 657–662. Vibration analysis of horizontally curved beams with warping using DQM.

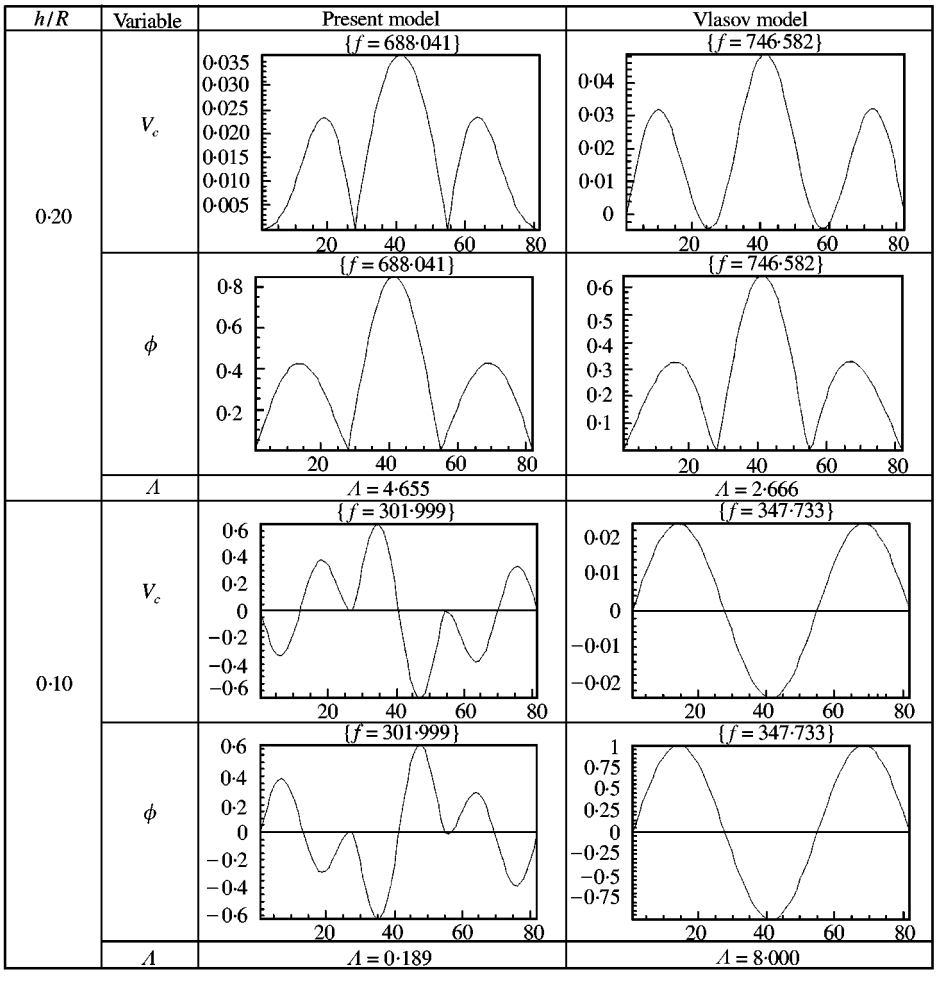

Figure 11. Mode shapes of the sixth frequency (f_6) for the beam with closed section, $\alpha = 180°$ and SS–SS outer boundary conditions Λ: measure of motion characteristics; v_c: vertical displacement, ϕ: torsion angle.

5. M. KAWAKAMI, T. SAKIYAMA *et al.* 1995 *Journal of Sound and Vibration* **187**, 381–401. In-plane and out-of-plane vibrations of curved beams with variable sections.
6. C. C. FU and Y. T. HSU 1995 *Computers and Structures* **54**, 147–159. The development of an improved curvilinear thin-walled Vlasov element.
7. A. S. GENDY and A. F. SALEEB 1994 *Journal of Sound and Vibration* **174**, 261–274. Vibration analysis of coupled extensional/flexural/torsional modes in curved beams with arbitrary thin walled sections.
8. V. H. CORTÍNEZ, M. T. PIOVAN and R. E. ROSSI 1999 *Structural Engineering and Mechanics*, **8**, 257–272. Out of plane vibrations of thin walled curved beams considering shear flexibility.
9. V. H. CORTÍNEZ, M. T. PIOVAN and R. H. GUTIERREZ 1999 *Proceedings of* VI *Pan American Congress of Applied Mechanics, Rio de Janeiro, Brazil.* Analytical solution for out of plane vibrations of shear deformable thin walled curved beams with pinned ends.
10. M. T. PIOVAN, V. H. CORTÍNEZ and R. E. ROSSI 1998 *Computational Mechanics* (E. Oñate and S. R. Idelsohn, editors). Barcelona, Spain: CIMNE. Vibrations of curved I beams with allowance for shear deformability.
11. C. P. HEINS and M. A. SABIN 1979 *Journal of the Structural Division ASCE* **105**, 2591–2600. Natural frequency of curved box girder bridges.

12. J. F. WILSON, Y. WANG and I. THREFALL 1999 *Journal of Sound and Vibration* **222**, 563–576. Responses of near-optimal continuous horizontal curved beams to transit loads.
13. C. H. KOU, S. E. BENZLEY, J. Y. HUANG and D. A. FIRMAGE 1992 *Journal of Structural Engineering* **118**, 2890–2910. Free vibration analysis of curved thin walled grinder bridges.
14. V. H. CORTÍNEZ and R. E. ROSSI 1998 *Revista Internacional de Métodos Numéricos para Cálculo y Diseño en Ingeniería* **14**, 293–316. Dinámica de vigas de sección abierta de pared delgada deformables por corte sujetas a un estado inicial de tensiones.
15. S. KRENK and O. GUNNESKOV 1981 *International Journal for Numerical Methods in Engineering* **17**, 1407–1426. Statics of thin-walled pretwisted beams.
16. Y. B. YANG and S. R. KUO 1987 *Journal of Structural Engineering* **113**, 1185–1202. Effect of curvature on stability of curved beams.
17. V. H. CORTÍNEZ and R. E. ROSSI 1998 *Computational Mechanics* (E. Oñate and S. R. Idelsohn, editors). Barcelona, Spain: CIMNE. Vibrations of pretwisted thin-walled beams with allowance for shear deformability.